仮想ダイポールレイヤーを用いた
時空間高精度脳機能マッピング

（課題番号　１３４８０２９１）

平成１３年度～平成１５年度科学研究費補助金
基盤研究(B)(2)研究成果報告書

平成１６年５月

堀　　潤　一
（新潟大学工学部助教授）

はしがき

本報告書は，平成１３年度～平成１５年度科学研究費補助金基盤研究(B)(2)の補助の下で実施された研究課題「仮想ダイポールレイヤーを用いた時空間高精度脳機能マッピング」（課題番号　１３４８０２９１）の成果をまとめたものである．

本研究プロジェクトは，1999年10月より2000年8月までの10ヶ月間のイリノイ大学シカゴ校における在外研究よりスタートする．受け入れ先である Biomedical Functional Imaging and Computing Laboratory のディレクタ Bin He 教授と間で，脳機能イメージング，特に脳の逆問題に関する共同研究を実施した．在外研究期間中の成果を更に発展させるためには，多チャンネルディジタル脳波計を軸とした実験設備の構築と海外共同研究先との打合せなどが不可欠であった．そこで，上記の研究課題を設定し，科学研究費補助金を得ることにより，ある程度の成果をあげることができた．本研究プロジェクトの主な成果は，下記の参考論文に記載されている．本報告書は，この論文を中心として再編集することによりまとめている．

Hori, J., Aiba, M., and He, B.: "Spatio-temporal dipole source imaging of brain electrical activity by means of time-varying parametric projection filter," IEEE Trans. Biomed. Eng.., (in press)

本研究を実施するに当たり，海外共同研究者であるイリノイ大学シカゴ校（現在ミネソタ大学）の Bin He 教授，イリノイ大学シカゴ校博士課程学生 Jie Lian 氏にさまざまな面で協力いただいた．また，実験などで新潟大学工学部福祉人間工学科斉藤・堀研究室の学生諸氏に手伝っていただいた．ここに感謝の意を表す．

平成16年5月

研究代表者　堀　潤一
（新潟大学工学部助教授）

平成１３年度～平成１５年度科学研究費補助金基盤研究(B)(2)研究成果報告書

研究課題名

仮想ダイポールレイヤーを用いた時空間高精度脳機能マッピング

（課題番号　１３４８０２９１）

研究組織

研究代表者　　　堀　　潤一（新潟大学工学部助教授）

海外共同研究者　Bin　　He (イリノイ大学シカゴ校助教授

（現在　ミネソタ大学教授））

交付決定額（配分額）

（金額単位：千円）

	直接経費	間接経費	合　計
平成 13 年度	9,400	0	9,400
平成 14 年度	2,700	0	2,700
平成 15 年度	1,200	0	1,200
総　計	13,300	0	13,300

研究発表

（１）学会誌等

1. Hori, J. and He, B., Equivalent dipole source imaging of brain electric activity by means of parametric projection filter, Annals of Biomedical Engineering, vol.29, no.5, pp.436-445, 2001.
2. Hori, J. and He, B.,EEG Cortical potential imaging of brain electrical activity by means of parametric projection filters, IEICE Trans. Info. & Syst., vol.E86-D, no.9, pp.1909-1920, Sept. 2003.
3. Hori, J., Lian, J., and He, B., Cortical potential imaging of brain electrical activity by means of parametric projection filter, Methods Inform. Med., vol.43, no.1, pp.66-69, March 2004.
4. Hori, J., Aiba, M., and He, B.: "Spatio-temporal dipole source imaging of brain electrical activity by means of time-varying parametric projection filter," IEEE Trans. Biomed. Eng.., (in press)

（2）口頭発表

1. 堀潤一，B. He, 等価ダイポールレイヤーによる脳機能解析，第 40 回日本 ME 学会大会，May 2001.
2. Hori, J. and He, B., High-resolution cortical imaging by means of parametric projection filters, 2001 Asia-Pacific Radio Science Conference, 205, Tokyo, Aug. 2001 (invited).
3. 宮田治，堀潤一，ダイポールイメージングによる脳内信号源の推定，信学技報，MBE2001-74, pp.23-30, Oct. 2001.
4. 相場雅彰，堀潤一，斉藤義明，B. He，時系列脳波マッピングの逆問題における瞬目アーチファクトの低減，第 11 回電気学会東京支部新潟支所研究発表会, p.78, Nov. 2001
5. 堀潤一，宮田治，斉藤義明，脳波等価ダイポールイメージングによる脳内信号源の推定，第 41 回日本 ME 学会大会，p.366, May 2002.
6. Hori, J., Lian, J., and He, B., Cortical potential imaging of brain electrical activity by means of parametric projection filter, Proc. 4th Int. Workshop Biosignal Interpretation, vol.4, 311-314, Italy, June 2002.
7. Hori, J. and He, B., Brain electrical imaging by means of parametric projection filters, Proc. Progress In Electromagnetic Research Symposium, Boston, July 2002 (invited).
8. 大類稔，堀潤一，斉藤義明，B. He，信号と雑音の統計的性質を考慮した空間逆フィルタによる脳内ダイポールイメージング日本 ME 学会甲信越支部・北陸支部合同大会，pp.12-13, Aug. 2002.
9. 桑原由希，堀潤一，斉藤義明，客観的聴覚評価のための聴性脳幹反応(ABR)の自動解析の検討，日本 ME 学会甲信越支部・北陸支部合同大会，pp.16-17, Aug. 2002.
10. 相場雅彰，堀潤一，斉藤義明，相場雅彰，パラメトリック射影フィルタを用いた時空間脳内ダイポールイメージング, 日本 ME 学会甲信越支部・北陸支部合同大会, pp.27-28, Aug. 2002.
11. Hori, J., Lian, J., and He, B., Comparison between parametric Weiner filter and parametric projection filter in cortical equivalent dipole layer imaging,Proc. 2nd Joint EMBS/BMES Conf., vol.2, 929-930, Houston, Oct. 2002.
12. 堀潤一, 脳内電気活動イメージングとその応用，第 12 回電気学会東京支部東京支部新潟支所研究発表会，pp.9-10, Nov. 2002（招待講演）.
13. 相場雅彰，堀潤一，斉藤義明，B. He，時空間脳内ダイポールイメージングにおける瞬目アーチファクトの低減, 第 12 回電気学会東京支部東京支部新潟支所研究発表会, p.52, Nov. 2002.
14. 徳武篤史，堀潤一，斉藤義明，多チャンネル生体信号を用いた情報インタフェースに

関する基礎研究，日本ME学会平成14年度専門別研究会　第3回医療・福祉におけるヒューマンインタフェース研究会, March 2003.

15. 堀潤一，相場雅彰，斉藤義明，B. He，雑音情報を取り入れた時空間脳内ダイポールイメージング，第5回日本ヒト脳機能マッピング学会大会抄録集，p.72, March 2003.
16. 堀潤一，相場雅彰，斉藤義明，B. He，時変性射影フィルタを用いた時空間脳内ダイポールイメージング，第42回日本ME学会大会，June 2003.
17. Hori, J., Aiba, M., and He, B., Spatio-temporal cortical equivalent dipole layer imaging by means of time-varying parametric projection filter, World Congress on Medical Physics and Biomedical Engineering, Sydney, Aug. 2003.
18. 桑原由希，堀潤一，斉藤義明，聴性脳幹反応(ABR)における加算平均処理の改善，信学技報，MBE2003-59, pp.19-24, Sept. 2003.
19. Hori, J., Aiba, M., Saitoh, Y., and He, B., Spatio-temporal brain electrical imaging based on time-varying spatial inverse filter, Proc. Progress in Electromagnetic Research Symposium, p.518, Hawaii, Oct. 2003.
20. 大島健志，堀潤一，斉藤義明，B. He，脳内ダイポールイメージングシステムの開発と誘発脳波への応用，第18回生体・生理工学シンポジウム論文集，pp.247-248, Oct. 2003.
21. Hori, J. and He, B.: "Artifact elimination in spatiotemporal cortical dipole layer imaging with parametric projection filter," 15th World Congress of the International Society of Brain Electromagnetic Topography, Urayasu, April 2004 (accepted).

（3）出版物

1. He, B., Hori, J., and Babiloni, F. Edited by Akay, M., Inverse EEG in Wiley Encyclopedia of Biomedical Engineering, John Wiley & Sons, Inc., (in press).

研究成果による工業所有権の出願・取得状況

なし

目次

ABSTRACT

In the present study, we explore suitable spatio-temporal filters for inverse estimation of an equivalent dipole-layer distribution from the scalp EEG for imaging of brain electric sources. We propose a time-varying parametric projection filter (tPPF) for the spatio-temporal EEG analysis. The performance of this tPPF algorithm was evaluated by computer simulation studies. An inhomogeneous three-concentric-spheres model was used in the present simulation study to represent the head volume conductor. An equivalent dipole layer was used to represent equivalently brain electric sources and estimated from the scalp potentials. The tPPF filter was tested to remove time-varying noise such as instantaneous artifacts caused by eyes-blink. The present simulation results indicate that the proposed time-variant tPPF method provides enhanced performance in rejecting time-varying noise, as compared with the time-invariant parametric projection filter.

INDEX TERMS

High-resolution EEG, Inverse problem, Spatio-temporal inverse filter, Equivalent dipole sources, Parametric projection filter, Eyes blink artifact elimination

I. INTRODUCTION

Brain electrical activity is spatially distributed in three dimensions of the brain and evolves in time. It is of importance to obtain spatio-temporal information regarding brain electrical activity from noninvasive electromagnetic measurements. Because of inherit high temporal resolution of electroencephalogram (EEG) measurements, high resolution EEG imaging, which aims at improving the spatial resolution of the EEG modalities, has received considerable attention in the past decades. Such EEG imaging modalities would facilitate noninvasive localization of foci of epileptic discharges in the brain, and the characterization of rapidly changing patterns of brain activation.

A number of efforts have been made to achieve high resolution EEG imaging. Among them of interest is the spatial enhancement approach, which attempts to deconvolve the low-pass spatial filtering effect of volume conduction of the head [1]-[22]. Cortical dipole layer imaging technique (CDIT), which attempts to estimate the cortical dipole distribution from the scalp potentials, is one of the spatial enhancement techniques. In this approach, an equivalent dipole source layer is used to model brain electrical activity and has been shown to provide enhanced performance in imaging brain electrical sources as compared with the smeared scalp EEG [4], [19], [22].

It is important to infer the origins from the scalp-recorded EEG, and to image the sources that generate the observed EEG on the scalp. Such a problem is usually called the inverse problem. The inverse problem of EEG is ill-posed and in general a regularization procedure is needed in order to obtain stable inverse solutions. Many regularization strategies, such as the generalized inverse with truncated singular value decomposition (TSVD), constrained least square method, and Tikhonov regularization method, have been proposed for solving the ill-conditioned inverse problem. Additive noise such as the uniform Gaussian white noise (GWN) is usually used to evaluate the performance of the inverse solutions using the above regularization procedures. On the other hand, the noise existing in scalp EEG measurements maybe non-uniformly distributed because of the variation in the electrode impedance and experimental environment. Several methods have been developed to handle the non-uniform noise. A multiple signal classification (MUSIC) algorithm [23] that incorporates a covariance matrix of background activity has been proposed for the MEG inverse problem [24]. Moreover, the linearly constrained minimum variance filter uses the noise covariance for dipole localization [25]. We have previously developed the parametric projection filter (PPF) based cortical dipole layer imaging technique, which allows estimating cortical dipole layer inverse solutions in the presence of noise covariance [19]. Our previous results indicate that the results of the PPF provide better approximation to the original dipole layer distribution than that of traditional inverse techniques in the case of low correlation between signal and noise distributions.

In the present study, we have expanded the PPF inverse spatial filter to the time-varying filter in order to handle the spatio-temporally varying nature of brain electrical activity. Concretely, the noise covariance and the regularization parameter of the PPF are supposed to be time-variant because the signal and noise are time-variant in EEG measurements. In the proposed approach, the information on the noise structure, as defined by the covariance matrix, is estimated from the spatial information of noise ensemble. We have applied this approach to perform the inverse regularization in equivalent dipole layer source imaging, and tested the proposed method in effectively rejecting time-variant artifact such as eyes blink artifact under the background noise. The proposed method will be applicable to non-averaged single trial data. After eliminating the time-variant noise, the data can also be averaged in order to suppress the background noise for analyzing the spatiotemporal behavior of brain electrical activity. The performance of the proposed time-variant PPF (tPPF) has been evaluated by computer simulations, as compared with time-invariant PPF.

II. METHODS

A. Spatio-temporal Dipole Layer Source Imaging

The observation system of brain electrical activity on the scalp shall be defined by the following equation:

$$g_k = A f_k + n_k \ (k = 1, \ldots, K) \tag{1}$$

where f_k is the vector of the equivalent source distribution of a dipole layer (DL), n_k is the vector of the additive noise and g_k is the vector of scalp-recorded potentials. Subscript k indicates the time instant. A denotes the transfer matrix from the equivalent source to the scalp potentials. In the present approach, f_k is the strength of the DL. In (1), we suppose that the signal f_k and noise n_k are time-variant while the transfer matrix A is time-invariant.

It is important to infer the origins from the scalp-recorded EEG, and to image the sources that generate the observed EEG on the scalp. The inverse process shall be defined by

$$f_{0k} = B_k g_k \tag{2}$$

where B_k is the spatio-temporal restoration filter and f_{0k} is the estimated source distribution of the DL. As the number of measurement electrodes is always smaller than the dimension of the unknown vector f_k, this problem is an underdetermined inverse problem. If the statistical information of the noise or signal are known or are estimated in accuracy, the restorative ability of the restoration filter B_k should be improved by using not only the transfer function A but also the signal and noise information. Therefore, the restoration filter B_k should be time variant system despite of the time invariant transfer function A because the signal f_k and noise n_k are time variant in (2). The details of the restoration filter B_k are described in Section II. B.

In the present simulation study, the head volume conductor is approximated by the inhomogeneous three-concentric-spheres model [26]. This head model takes the variation in conductivity of different tissues, such as the scalp, the skull and the brain, into consideration. An equivalent DL is assumed within the brain sphere being concentric to the cortical surface. Radial current dipoles are uniformly distributed over the spherical DL to simulate brain electrical sources accounting for the scalp potentials.

By using the DL distribution, the electrical sources inside of the DL sphere are equivalently represented by the DL surrounding the sources, regardless of the number or the direction of the dipole sources [22]. That is, the DL model used in the present study is an equivalent source model, which shall account for arbitrary source configurations within the DL [22]. The transfer function from the DL to the scalp potentials is obtained by considering the geometry of the model and physical relationship between the quantities involved. The strength of the DL is estimated from the noise-contaminated scalp potentials.

B. Time-Varying Parametric Projection Filter

The general inverse, which is also called the Moore-Penrose pseudoinverse, denoted by A^+, minimizes the norm of the restored DL distribution f_{0k} under the constraint $g_k = A f_{0k}$ in the absence of noise. In practice, singular value decomposition (SVD) can be used to calculate A^+ [27], [28]. In the presence of noise, the truncated SVD and various regularization techniques have been implemented in order to reduce the effect of noise [29].

When the statistical information of signal and noise are presented, the Wiener filter can be applied to the inverse problem [30], [4], [8]. Suppose R_k and Q_k the signal and the noise covariance, which can be derived from the expectation over the signal $\{f\}$ and noise $\{n\}$ ensemble, $E[f f^*]$ and $E[n\, n^*]$, respectively. f^* and n^* are the transpose of f and n, respectively. The parametric Wiener filter (PWF) is derived by

$$B_k = R_k A^* (A R_k A^* + \gamma_k Q_k)^{-1}. \tag{3}$$

with γ_k a small positive number known as the regularization parameter, and A^* is the transpose matrix of A. If $R_k = Q_k = I$ (the identity matrix), then equation (3) is reduced to the zero-order Tikhonov regularization method [31]. The PWF has been applied to brain source imaging [4], [8]. However, it is difficult to obtain the signal covariance, R_k. Moreover, even if the signal covariance is obtained, the filter may not provide satisfactory performance for non-periodic abnormal signals, which is obviously different from the expectation of signals.

To overcome this problem, the PPF has been introduced to solve the inverse problem [32]. The PPF is derived by [32], [19]

$$B_k = A^* (A A^* + \gamma_k Q_k)^{-1}. \tag{4}$$

The PPF considers just the covariance matrix of the noise distribution, Q_k, that is, $R_k = I$ in (3). The PPF, using the free parameter, can improve the restorative ability from the projection filter, which provides the orthogonal projection of the original signal onto the range of the restoration filter that minimizes the expectation over the noise component in the restored signal. The scalar parameter $\gamma_k > 0$ in (4) controls the mutual weights of two error terms. The determination of the value of parameter γ_k is left to the subjective judgment of the user. We have applied the time-invariant version of the PPF, which is described by omitting the time k in (4), to the cortical dipole layer source imaging [19]. The time-variant PPF (tPPF) can also be applied to the spatio-temporal inverse problem described by (2). The optimum choice for γ_k and Q_k are described in II. C and II. D, respectively.

C. Estimation of Regularization Parameter

The tPPF has a free parameter that determines the restorative ability. The optimum parameter of the tPPF for the best approximation should be determined by minimizing the relative error (RE) between the actual DL distribution and the estimated DL distribution as

$$\mathrm{RE}_k = \| f_k - f_{0k} \| / \| f_k \| \tag{5}$$

in every time instance, k. Unfortunately, the original DL distribution, f_k, could not be obtained under practical conditions. If a signal covariance R can be estimated, we can use the parametric Wiener filter in (3). When minimizing $E_n \| f_k - f_{0k} \|^2$, the regularization parameter γ in (3) must be 1. We consider the restoration filter in the absence of any signal information. In that case, we have to estimate the value of the regularization parameter in order to control the signal and noise amplitudes. We have developed a new criterion for determining the optimum parameter without knowing the original DL distribution. One possibility is to use the following cost function:

$$\begin{aligned} J(\gamma_k) &= E_n \| f_{0k} - B_k (A f_{0k} + n_k) \|^2 \\ &= \| f_{0k} - B_k A f_{0k} \|^2 + tr(B_k Q B_k^*) + 2\,(f_{0k} - B_k A f_{0k},\, B_k g_k - B_k A f_{0k}) \end{aligned} \tag{6}$$

where f_{0k} is the restored DL distribution using an initial value for γ_k, which should be relatively large to reduce the effect of additive noise on the coefficients. Concretely, γ can be selected when the second term in (6), which represents the amplitude of noise in the restored plane, is sufficiently small. Equation (6) is approximate to the squared error between f_k and f_{0k} in taking an expectation of noise without knowing the original DL distribution f_k. The first term and the second term correspond to the squared restorative error and squared restored noise, respectively. And the third term corresponds to the inner product between the restorative error and the restored noise. In the previous parameter determination procedure developed in [19], the third term in (6) was neglected. In the present study, this term was kept in (6), and it will slightly improve the inverse results because the correlation between signal and noise is negligible. Furthermore, the following procedure provides the optimum approximation of parameter γ_k: (i) Compute the restored DL distribution f_{0k} using an initial value of γ_k, (ii) Calculate the evaluation function $J(\gamma_k)$, (iii) Obtain new optimum parameter γ_{1k} that minimizes $J(\gamma_k)$, (iv) Repeat (i)–(iii) replacing γ_k with the new γ_{1k} until $\|\gamma_k - \gamma_{1k}\| / \|\gamma_k\| < e$ where e is the condition of convergence, which guarantees that, at the least, the order of magnitude of the squared error between f_k and f_{0k} should be correct. The present computer simulation indicates that this procedure also provides the unique solution of γ_k despite of varying the initial value. This method is applicable not only for the tPPF but also for other parametric inverse techniques such as the TSVD, the Tikhonov regularization, the constrained least-square method, and the PWF [32].

D. Estimation of Noise Covariance

If there is no spontaneous artifact in the series of EEG measurements, the noise covariance Q_k should be constant and it may be estimated from data that is known to be source free, such as pre-stimulus data in evoked potentials in a clinical situation [24], [25]. If there are some artifacts, Q_k should be adaptive to the spatial distribution of the artifacts in order to suppress them. In the present study, two types of noise covariance are applied to the tPPF. One is the noise covariance for background noise, denoted by Q_b. Time invariant background noise covariance Q_b might be estimated from the pre stimulus evoked potentials that do not include signals. And the other is the noise covariance for instantaneous artifact such as eyes blink, denoted by Q_a. The eyes blink covariance Q_a is substituted by the voluntary wink data. The eyes blink artifacts may be eliminated by using two types of noise covariance in the tPPF according to the signal conditions with or without artifacts.

In order to apply the noise covariance to the tPPF, the time intervals of the eyes blink should be estimated. The template of potential distribution in the case of eyes blink is measured by voluntary wink data in advance. And the correlation coefficients ρ_k ($k = 1, \ldots, K$) between each scalp potential distribution and the eyes blink template are calculated in every time course. The time-interval of eyes blink is estimated by the correlation coefficient that is larger than the threshold that is settled by experience. Finally, the noise covariance of the tPPF is determined by the following equation:

$$Q_k = \begin{cases} Q_b & \rho_k \leq threshold \\ Q_a & \rho_k > threshold \end{cases} \tag{7}$$

E. Simulation Protocol

In the present simulation, two or four dipole sources were used to represent multiple localized brain electrical sources. The dipoles were oriented radially or tangentially to the sphere with varying strengths. The strength of each dipole is changed from -1 to 1 with sinusoid in time. In the case of two dipole sources, the frequencies of fluctuation in the dipole moments were set to 10 Hz and 30 Hz that assuming EEG alpha and gamma activities, respectively. In the case of four dipole sources, the frequencies of them were set to 10 Hz, 20 Hz, 30 Hz, and 40 Hz.

In the present study, the source-conductor model [11], [13], [16] as shown in Fig. 1, was used. In this model, the radii of the brain, r_1, the skull, r_2, and the scalp, R, spheres were taken as 0.87, 0.92, and 1.0, respectively [26], [11]. The normalized conductivity of the scalp and the brain was taken as $\sigma_0 = 1.0$, and that of the skull as $\sigma_s=$ 0.0125. The potentials on the scalp surface, generated by current dipoles inside the brain, can be calculated by solving the forward problem from the dipole source to the scalp-surface potential [33]. The strength of the DL can be calculated by solving the forward problem from the assumed dipole source to the equivalent DL strength [22].

Two kinds of additive noise were considered. One is the time invariant noise such as a background noise that stochastic characteristics do not change in time. The time invariant background noise is expressed by Gaussian white noise (GWN). The noise level defined as the ratio between the norm of noise and the averaged norm of the simulated scalp potential over time was set to 0.1. The other is the time variant noise such as eyes blink artifacts. The movements of eyeballs generate electrical artifacts because the cornea sides of each eyeball are positively electrical-charged against the retina sides. The eyes blink artifacts appear as spike-like shape at upper parts of the eyes with the time duration of about 0.3 s. Since the amplitude of the eyes blink artifacts is at the order of 100 μV that is much greater than ordinary scalp potentials, the scalp measured potentials are degraded by the eyes blink artifacts. The simulated artifact is represented in space and time domain as Figs. 2 (a) and (b), respectively. The amplitude of the artifact was set to two times of the maximum of the scalp potentials. The duration of the artifact was set to 0.3 s. Figure 2(c) shows the time series of correlation coefficients between a template eyes blink artifact distribution and scalp potential distributions. The template artifact was obtained with a simulated wink data, which has the same distribution as that of the eye blink artifact and was distorted with the GWN generated with a different seed in advance. As shown in Fig. 2(c), the correlation coefficient is high while the eyes blink occurred.

III. Results

A DL with 1280 radial dipoles at a radius of 0.8 was used, according to the previous simulation results [11]. The scalp potential distribution was observed from 128 positions over the upper hemisphere scalp. The GWN with the noise level of 0.1 was added to the scalp potentials to simulate noise-contaminated scalp EEG measurements. Sampling rate was set to 100 Hz. The estimated results of our simulation were evaluated with the RE between the actual and estimated DL distribution in addition to visual description of the DL distributions since the DL distribution presents not only the information on the locations of the dipole sources but also on the directions of them.

First of all, the time-invariant PPF, with the constant noise covariance $Q_k = Q_b$ and the constant regularization parameter $\gamma_k = \gamma_{ave}$, was applied to estimate DL distributions f_k ($k = 1, \ldots, K$). Q_b was estimated from the background activity and it was set to the same in every time instant. γ_{ave} was calculated by minimizing the average of RE over time. Figure 3(a) shows the simulated eyes blink artifact over the scalp and Fig. 3(b) shows the RE between the actual and estimated DL distribution in time sequence in the case of two radial dipole sources at the eccentricity of 0.6. Because the generalization parameter γ_{ave} of inverse filtering was fixed, the RE was large over the entire time period. In addition, the RE during the blinking exercise became extremely large because the noise covariance of the restoration filter during the artifact was as same as that of the background noise activity though the statistical characteristics of artifact noise was highly different from the background noise. The averages of the RE for the background noise and eyes blink noise were 0.685 and 1.067, respectively. The estimated distribution of DL varied substantially from the actual DL distribution in both the background noise and eyes blink.

Next, we applied the restoration filter with time varying regularization parameter γ_k. The noise covariance, which was calculated with the background noise activity, was constant in every time instant ($Q_k = Q_b$). Fig. 3(c) shows the time series of RE between the actual and estimated DL distribution. The RE during the eyes blinking exercise was large while that during the background noise was reduced due to the use of time varying parameter γ_k. The averages of the RE for the background noise and eyes blink noise were improved to 0.530 and 0.978, respectively. The estimated DL distributions during the background noise were better than those obtained by using the time invariant regularization parameter. However, the DL distributions during the eyes blink remained unchanged since the statistical information on the eyes blink artifact was not taken into account in the calculation.

Moreover, the restoration with constant noise covariance of eyes blink artifact ($Q_k = Q_a$) was applied to the DL estimation. The result is shown in Fig. 3(d). The averages of the RE for the background noise and eyes blink noise were 0.640 and 0.637, respectively. The RE during the eyes blinking exercise became smaller than Fig. 3(c). However the RE for background noise became larger.

Finally, the restoration filter with the time varying parameter γ_k and the time varying noise covariance Q_k was applied to the spatio-temporal inverse problem. Two types of noise covariance, of the background noise and eyes blink artifact, were used to estimate cortical DL from the scalp potentials with or without the eyes blink artifact. Fig. 3(e) shows the time series of RE. The RE during the eyes blink exercises was reduced by using the noise covariance of the eyes blink template. The averages of the RE for the background noise and eyes blink noise were reduced to 0.530 and 0.637, respectively. The difference between Figs. 3 (d) and (e) looks small, but the DL map corresponding to the case shown in Fig. 3 (d) was noisier than that of Fig. 3 (e) in the absence of artifact (The DL maps are shown in Fig. 8).

We confirmed the restorative ability of tPPF for time-varying DL imaging. The estimated DL strengths using the time invariant and time variant noise covariance were compared at the nearest point in space from an assumed dipole source of 10 Hz. Figure 4(a) shows the normalized strength of the actual DL at the nearest point from an assumed dipole source of 10 Hz in the case of two radial dipole sources at the eccentricity of 0.7. The waveform of the source strength at the point was similar to the sinusoidal wave of 10 Hz. Figure 4(b) shows the normalized scalp potential at the nearest point from an assumed dipole source of 10 Hz. The scalp potential was contaminated with the background GWN and the waveform was overlapped with that of the other dipole source of 30Hz sinusoidal wave. Figures 4 (c)-(e) show estimated results of the DL strength by the PPF with time invariant γ_k and Q_b of background noise, time variant γ_k and time invariant Q_b, and time variant γ_k and Q_k, respectively. The position of the DL strength is the same as Fig. 4(a). The time variant regularization parameter γ_k was estimated in every time instant in Figs. (d) and (e). The distortion around the eyes blinking artifact of the time-variant Q_k in Fig. 4(e) became small as compared with that of the time-invariant Q_k in Figs. 4 (c) and (d). The amplitude of the estimated signal in Fig. 4 (c) looks stable in spite of artifact existing because γ_k and Q_k are constant. If γ_k was estimated to minimize the cost function in every time, the amplitude became small during artifact in Fig. 4 (d) in order to suppress the artifact noise. As results, Fig. 4 (c) looks better than Fig. 4 (d). On the other hand, when considering artifact by using time varying Q_k, the signal became stable in Fig. 4 (e).

Figure 5(a) shows one example of the actual DL distribution of two radial dipoles at a single time point during the artifact. The dipole sources were located at the eccentricity of 0.7 with the angle of $\pi/3$. Figure 5(b) shows the scalp potential distribution contaminated with eyes blink artifact as shown in Fig. 2. Figures 5 (c), (d), and (e) show estimated inverse results of the DL using the PPF with time invariant γ_k and Q_k, time variant γ_k and time invariant Q_k, and time variant γ_k and Q_k, respectively, which are normalized by the maximum of the actual DL distribution. As shown in Figs. 5(c)-(d), the DL distribution obtained by the time-invariant Q_k was blurred and large distortion in the amplitude of the DL distribution observed. Owing to the strong artifact noise, the restoration filter was going to suppress both the DL distribution and the noise. As a result, the DL distribution was contaminated with noise. On the other hand, the DL distribution obtained by the tPPF shows two areas of well-localized activity similar to the actual DL source distribution (Fig. 5(a)). This result is consistent with the temporal performance of the tPPF as shown in Fig. 3(e). The difference between the two inverse techniques is the noise covariance that was utilized in the PPF. These results show that the present tPPF filter can suppress the eyes blink artifact by using the noise covariance of the eyes blink artifact.

Figure 6 shows another example of DL estimation in the case of two tangential dipoles at the eccentricity of 0.7 with an angle of $\pi/3$. The improved performance of the tPPF (e) as compared with the time-invariant inverse filters (c) and (d) despite the direction of dipoles is shown in Fig. 6. As shown in Figs. 6(c)-(d), the DL distribution obtained by the time-invariant Q_k was blurred and failed to reconstruct the distribution of DL. On the other hand, the DL distribution obtained by the tPPF shows good reconstruction of the spatial pattern of the DL distribution as compared with the actual DL distribution.

Figure 7 shows one example of DL estimation in the case of four radial dipoles at a single time point during the artifact. The positions of four dipoles are given as follows:

$$[\pm 0.75\sin(\pi/6), 0, 0.75\sin(\pi/6)]$$
$$[0, \pm 0.75\sin(\pi/6), 0.75\sin(\pi/6)]$$

Fig. 7(a) shows the distribution of the actual DL. Fig. 7(b) shows the scalp potential distribution by the 4 radial dipoles being contaminated by noise. Figs. 7(c)-(e) show the inverse estimation results. The extrema corresponding to the four radial dipoles are well reconstructed by the time-variant PPF as shown in Fig. 7(e). On the other hand, the time-invariant PPF resulted significant artifacts in the DL inverse solutions (Fig. 7(c) and (d)), not revealing the major features of the spatial pattern of the DL distribution.

Fig. 8 shows one example of cortical DL imaging of two tangential dipoles at the eccentricity of 0.7 with an angle of $\pi/3$. Background noise of 0.1 NSR was added to the scalp potentials. No eye-blink artifact was considered. The improved performance of time-varying regularization parameter γ_k is observed in Fig. 8(d) and Fig. 8(f). Note distortion in the DL topographic map in Fig. 8(e) due to use of the Q_a. The result using time varying regularization parameter γ_k and Q_k (and Q_b in this case) provided the best reconstruction result.

IV. DISCUSSION

A spatio-temporal inverse filter to solve the cortical inverse problem has been developed by taking the time-varying properties into consideration. The usefulness of this inverse filter has been tested in handling time-variant noise such as eyes blink artifacts. The present inverse filter has the time variant regularization parameter and the time variant noise covariance. The effect of the time variant regularization parameter on the DL inverse solution is shown in Figs. 3. The RE between the actual and estimated DL distributions was reduced in every time instant. Especially, the RE during the period with only the background noise was dramatically reduced. The present results suggest that the value of the regularization parameter should be changed according to the signal and noise configurations. Since the signal, that is, the DL distribution changes in every time instant, the regularization parameter γ_k of the tPPF should be changed even if the statistical characteristics of noise are constant.

Noise plays an important role in brain source imaging, as in any other ill-posed inverse problem. In the present study, we have investigated the performance of dipole source imaging by considering noise covariance matrix through the use of PPF in (4). The PPF consists of the noise covariance matrix that represents spatial information of noise distribution. It was reported that the PPF is effective for improving cortical dipole source imaging, under the condition of low correlation between the signal and noise distributions and has similar restorative ability to the GWN and the condition of high correlation between the signal and noise [19]. In the present simulation, the correlation between the signal and the eyes blink artifact is low because the major areas of activity in the scalp potentials are located at the parietal region while the eyes blink artifacts are located in the frontal regions, near the eye balls.

If we can obtain both signal covariance matrix and noise covariance, the PWF as shown in (3) may be applied to the inverse problem. There is no, to our knowledge, comprehensive investigation on cortical DL imaging in the metric of noise, in which non-white noise is considered. Actually, it is difficult to estimate the signal covariance exactly from the observed scalp potentials. Whenever the signal covariance is estimated, the PWF reconstructs the averaged signal over the time. We have confirmed the restorative ability of the PPF and the PWF in a separate study [34]. The simulation results obtained in that study suggest that, the PPF has better performance than other inverse filters under the condition of low correlation between signal and noise distributions. On the other hand, the PWF with incorporating signal information provides good results of equivalent dipole source imaging results compared to the PPF and Tikhonov regularization without signal covariance under the condition of high correlation between signal and noise distributions. As mentioned above, since the correlation between the eyes blink artifact and the brain electrical activities are low in most cases, we may use the PPF for eyes blink artifact suppression. If we can obtain the signal covariance in time course, the time-variant PWF would be also applicable to the equivalent cortical dipole layer imaging. In order to improve the resolution of restored dipole source imaging, we should choose the PPF and PWF according to the correlation between signal and noise distributions. The time variant PWF will be addressed in future investigation.

The signal space projection (SSP) method was applied for the detection and characterization of time dependent MEG data [35]-[36]. The projection operators used in the SSP divide the observed signals into the signal space and noise space. The SSP also used the spatial noise distribution in order to search and to remove artifacts. Inverse techniques used in the reported SSP studies were based on the SVD or pseudoinverse. Partial SSP that applies only in corrupted epochs due to eye blinks was also proposed [37]. In this later investigation, combination of temporal detection of eye blinks and SSP noise suppression was used so either the artifact be rejected based on temporal detection or SSP applied in order to extract useful spatial information [37]. On the other hand, the present time-varying spatio-temporal PPF approach incorporates time-variant noise distribution information so it provides a general framework to handle various noise and artifacts, including eye blinks, muscle noise, etc. By incorporating the statistical properties of noise distribution into the inverse imaging, the tPPF approach promises to handle various noise. Furthermore, we propose in the present tPPF approach to use the time-variant regularization parameter, which adjust the estimation error and the noise in the original signal space.

The effect of the time variant noise covariance was shown in Figs. 3(c) and (d). In the present simulation, two types of noise covariance were used. In the case of time-variant noise covariance, the RE during the period of the eyes blink artifact was reduced as compared with that in the case of time-invariant noise covariance. The present results suggest that the estimation was improved by changing the noise covariance in the situation of eyes blink artifacts. The effects of the time-variant noise covariance on the cortical dipole layer imaging are further illustrated in Figs. 5-7. In the space domain, Figs. 5-7 suggest the utility of the time-variant noise covariance in rejecting the artifacts like eyes blink. While using of noise covariance estimated from EEG data during eyes blink would suppress well the effects of artifact on the cortical imaging, using only the noise covariance of artifact will on the other hand distort the cortical imaging results when there exists only background noise, as shown in Fig. 8. Figs. 5-8 suggest that it is optimal to use the noise covariance being estimated from the EEG data at which moment the spatial source analysis is performed. In other word, it is desirable to use time-varying imaging instead of time-independent imaging.

In order to apply the time varying noise covariance, the time windows contaminated with eyes blink artifacts should be estimated in advance. The time windows were estimated by the threshold of the spatial correlation coefficients between the template of voluntary wink artifact distribution and the measured scalp potential distributions.

In the time variant PPF, the regularization parameter γ_k is calculated in ever time instant. It is time consuming to estimate an optimum value of the regularization parameter using the proposed iterating procedure. The number of iteration depends on the difference between the value of the initial parameter and that of the optimum parameter. Considering the sufficient sampling frequency in the time domain, the DL distribution at time instant k may be similar to that at time instant k-1. Then, by substituting the initial value for γ_k by γ_{k-1}, the parameter converged to the optimum value faster than the previous method.

In summary, we have developed a time-varying PPF inverse filter for cortical imaging, and showed its applicability in suppressing rapidly changing artifacts such as the eyes blink. The present simulation results suggest that the estimation error is reduced substantially by taking the spatio-temporal properties of the noise into consideration, such as eyes blink artifacts. Further investigations on other applications of this new method should be addressed in the future.

ACKNOWLEDGMENT

The authors would like to thank Dr. Jie Lian for useful discussions. This work was supported in part by NSF CAREER Award BES-9875344, Grant-In-Aid for Scientific Research from Japanese Society for the Promotion of Science No. 13480291, Grant for Promotion of Niigata University Research Projects, and NIH 1RO1EB00178.

References

[1] M. Hamalainen and R. Ilmoniemi, "Interpreting measured magnetic fields of the brain: estimates of current distributions," Univ. Helsinki, Finland Tech. Rep. TKK-F- A559, 1984.

[2] R. Sidman, M. Ford, G. Ramsey, and C. Schlichting, "Age-related features of the resting and P300 auditory evoked responses using the dipole localization method and cortical imaging technique," *J. Neurosci. Meth.*, vol. 33, pp. 23-32, 1990.

[3] J. Z. Wang, S. J. Williamnon, and L. Kaufman, "Magnetic source images determined by a lead-field analysis: The unique minimum-norm least-squares estimation," *IEEE Trans. Biomed. Eng.*, vol. 39, pp. 665-575, 1992.

[4] A. M. Dale and M. Sereno, "Improved localization of cortical activity by combining EEG and MEG with MRI cortical surface reconstruction: a linear approach," *J. Cognitive Neuroscience.*, vol. 5, pp. 162-176, 1993.

[5] R. Srebro, R. M. Oguz, K. Hughlett, and P. D. Purdy, "Estimating regional brain activity from evoked potential field on the scalp," *IEEE Trans. Biomed. Eng.*, vol. 40, pp. 509-516, 1993.

[6] A. Gevins, J. Le, N. K. Martin, P. Brickett, J. Desmond, and B. Reutter, "High resolution EEG: 124-channel recording, spatial deblurring and MRI integration methods," *Electroenceph. Clin. Neurophysiol*, vol. 90, pp. 337-358, 1994.

[7] P. Nunez, R. B. Silibertein, P. J. Cdush, R. S. Wijesinghe, A. F. Westdrop, and R. Srinivasan, "A theoretical and experimental study of high resolution EEG based on surface Laplacian and cortical imaging," *Electroenceph. and Clin. Neurophysiol.*, vol. 90, pp. 40-57, 1994.

[8] J. W. Philips, R. M. Leahy, J. C. Mosher, and B. Timsari, "Imaging neural electrical activity from MEG and EEG," *IEEE Trans. Med. Imaging.*, vol. 16, pp. 338-348, 1997.

[9] F. Babiloni, C. Babiloni, F. Carducci, L. Fattorini, C. Anello, P. Onorati, and A. Urbano, "High resolution EEG: a new model-dependent spatial deblurring method using a realistically-shaped MR-constructed subject's head model," *Electroenceph. Clin. Neurophysiol.*, vol. 102, pp. 69-80, 1997.

[10] S. Baillet and L. Garnero, "A Bayesian approach to introducing anatomo-functional priors in the EEG/MEG inverse problem," *IEEE Trans. Biomed. Eng.*, vol. 44, vol. 374-385, 1997.

[11] Y. Wang and B. He, "A computer simulation study of cortical imaging from scalp potentials," *IEEE Trans. Biomed. Eng.*, vol. 45, pp. 724-735, 1998.

[12] G. Edlinger, P. Wach, and G. Pfurtscheller, "On the realization of an analytic high-resolution EEG," *IEEE Trans. Biomed. Eng.*, vol. 45, pp. 736-45, 1998.

[13] B. He, "High resolution imaging of brain electrical sources," *IEEE Eng. Med. Biol.*, Sept./Oct., pp. 123-129, 1998.

[14] M. Fuchs, M. Wagner, T. Kohler, and H. A. Wischmann, "Linear and nonlinear current density reconstructions," *J. Clin. Neurophysiol.*, vol. 16, pp. 267-295, 1999.

[15] B. He, Y. Wang, and D. Wu, "Estimating cortical potentials from scalp EEG's in a realistically shaped inhomogeneous head model," *IEEE Trans. Biomed. Eng.*, vol. 46, pp. 1264-1268, 1999.

[16] B. He, "Brain Electric Source Imaging – Scalp Laplacian mapping and cortical imaging," *Crit. Rev. BME*, vol. 27, 149-188, 1999.

[17] B. He, J. Lian, K. M. Spencer, J. Dien, and E. Donchin, "A Cortical Potential Imaging Analysis of the P300 and Novelty P3 Components," *Human Brain Mapping*, vol. 12, pp. 120-130, 2001.

[18] J. Lian and B. He, "A Minimal Product Method and Its Application to Cortical Imaging," *Brain Topography*, 13:209-217, 2001.

[19] J. Hori and B. He, "Equivalent dipole source imaging of brain electric activity by means of parametric projection filter," *Annals Biomed. Eng.*, vol. 29, pp. 434-445, 2001.

[20] J.O. Ollikainen, M. Vauhkonen, P. A. Karjalainen, and J. P. Kaipio, "A new computational approach for cortical imaging," *IEEE Trans. Med. Imag.*, vol. 20, pp. 325-332, 2001.

[21] B. He, Z. Zhang, J. Lian, H. Sasaki, S. Wu, and V. L. Towle, "Boundary element method based cortical potential imaging of somatosensory evoked potentials using subjects' magnetic resonance images," *Neuroimage*, vol. 16, pp. 564-576, 2002.

[22] B. He, D. Yao, and J. Lian, "High resolution EEG: on the cortical equivalent dipole layer imaging," *Clinical Neurophysiology*, vol. 113, pp. 227-235, 2002.

[23] J. C. Mosher, P. S. Lewis, and R. M. Leahy, "Multiple dipole modeling and localization from spatio-temporal MEG data," *IEEE Trans. Biomed. Eng.*, vol. 39, pp. 541-557, 1992.

[24] K. Sekihara, D. Poeppel, A. Marantz, H. Koizumi, and Y. Miyashita, "Noise covariance incorporated MEG-MUSIC algorithm: A method for multiple-dipole estimation tolerant of the influence of background brain activity," *IEEE Trans. Biomed. Eng.*, vol. 44, pp. 839-847, 1997.

[25] B. D. Van Veen, W. V. Drongelen, M. Yuchtman, and A. Suzuki, "Localization of brain electrical activity via linearly constrained minimum variance spatial filtering," *IEEE Trans. Biomed. Eng.*, vol. 44, pp. 867-880, 1997.

[26] S. Rush and D. A. Driscoll, "EEG electrode sensitivity – An application of reciprocity," *IEEE Trans. Biomed. Eng.*, vol. BME-16, pp. 15-22, 1969.

[27] E. Biglieri and K. Yao, "Some properties of SVD and their application to digital signal processing," *Signal Proccessing.*, vol. 18, pp. 227-289, 1989.

[28] Y. S. Shim and Z. H. Cho, "SVD pseudo-inversion image reconstruction," *IEEE Trans. Acoust. Speech Signal Processing*, vol. 29, pp. 904-909, 1981.

[29] P. C. Hansen, "Truncated singular value decomposition solutions to discrete ill-posed problems with ill-determined numerical rank," *SIAM J. Sci. Stat. Comput.*, vol. 11, pp. 503-518, 1990.

[30] H. Ogawa and E. Oja, "Projection filter, Wiener filter, and Kahunen-Loeve subspaces in digital image processing. *J. Math. Anal. Appl.*, vol. 114, pp. 37-51, 1987.

[31] A. N. Tikhonov and V. Y. Arsenin, "*Solutions of ill-posed problems*," New York: Wiley, 1977.

[32] E. Oja and H. Ogawa, "Parametric projection filter for image and signal restoration," *IEEE Trans. Acoust. Speech, Signal Proccessing.*, vol. 34, pp. 1643-1653, 1986.

[33] R. N. Kavanagh, T. M. Darcey, D. Lehmann, and D. H. Fender, "Evaluation of methods for three-dimensional localization of electrical sources in the human brain," *IEEE Trans. Biomed. Eng.*, vol. BME-25, pp. 421-429, 1978.

[34] J. Hori, J. Lian, and B. He, "Comparison between parametric Weiner filter and parametric projection filter in cortical equivalent dipole layer imaging," *Proc. 2nd Joint EMBS/BMES Conf.*, pp. 929-930, Houston, Oct 2002.

[35] M. A. Uusitalo and R. J. Ilmoniemi, "The signal-space projection (SSP) method for separating MEG or EEG into components," *Med. Biol. Eng. Comput.*, vol. 35, pp. 135–140, 1997.

[36] G. Nolte and G. Curio, "The effect of artifact rejection by signal-space-projection on source localization accuracy in MEG measurements," *IEEE Biomed. Eng.*, vol. 46, pp. 400-408, 1999.

[37] G. Nolte and M. S. Hamalainen, "Partial signal space projection for artifact removal in MEG measurements: a theoretical analysis," *Phys. Med. Biol.*, vol. 46, pp. 2873-2887, 2001.

FIGURES

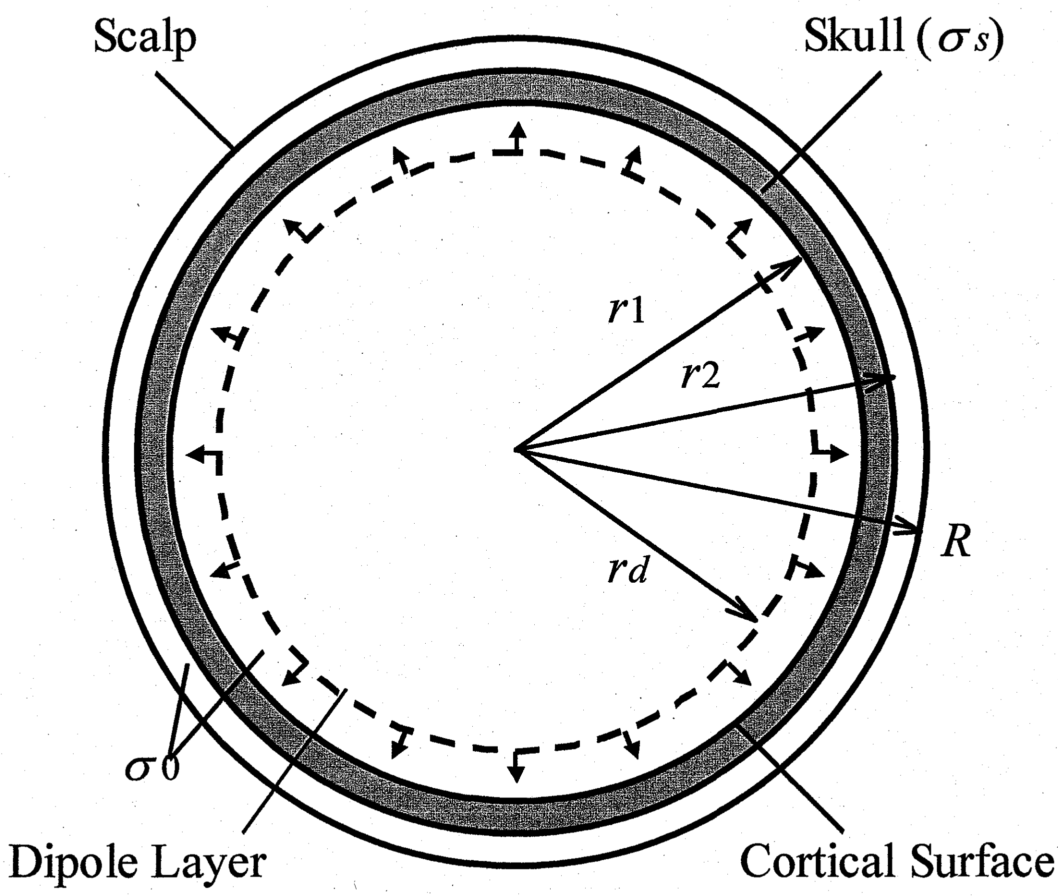

Fig. 1. Schematic illustration of the head volume conductor-source model. The head is represented by an inhomogeneous concentric three-sphere volume conductor model with radii r_1, r_2, and R being 0.87, 0.92, and 1.0, respectively. The normalized conductivity of the scalp and the brain is taken as 1.0, and that of the skull as 0.0125. Dipoles are uniformly distributed over a sphere with the radius of r_d.

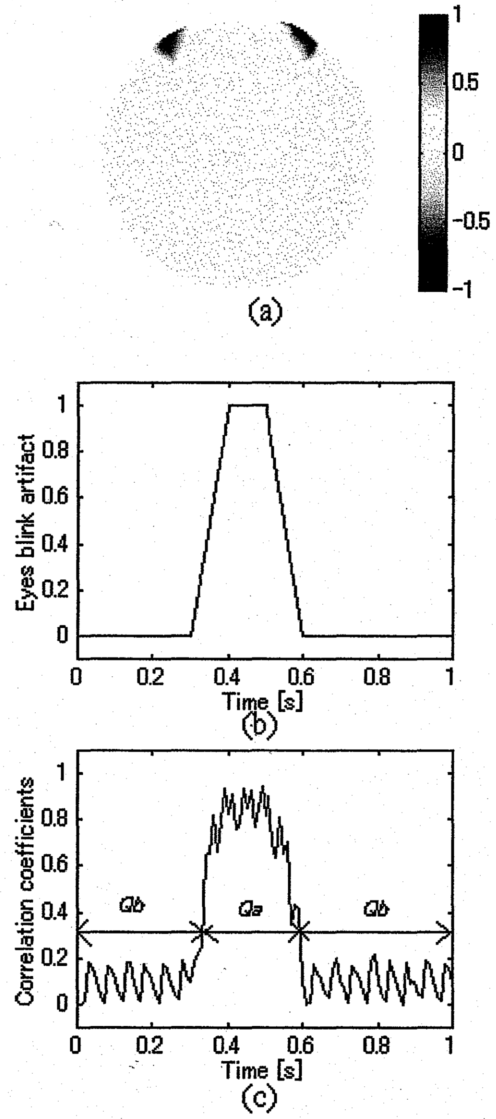

Fig. 2. Simulated eyes-blink artifact represented in (a) space and (b) time domain. The artifacts caused by eyes-blink appear in the frontal area over the scalp. And they continue about 0.3 seconds. (c) shows the time series of correlation coefficients between a template eyes blink artifact distribution and a scalp potential distribution.

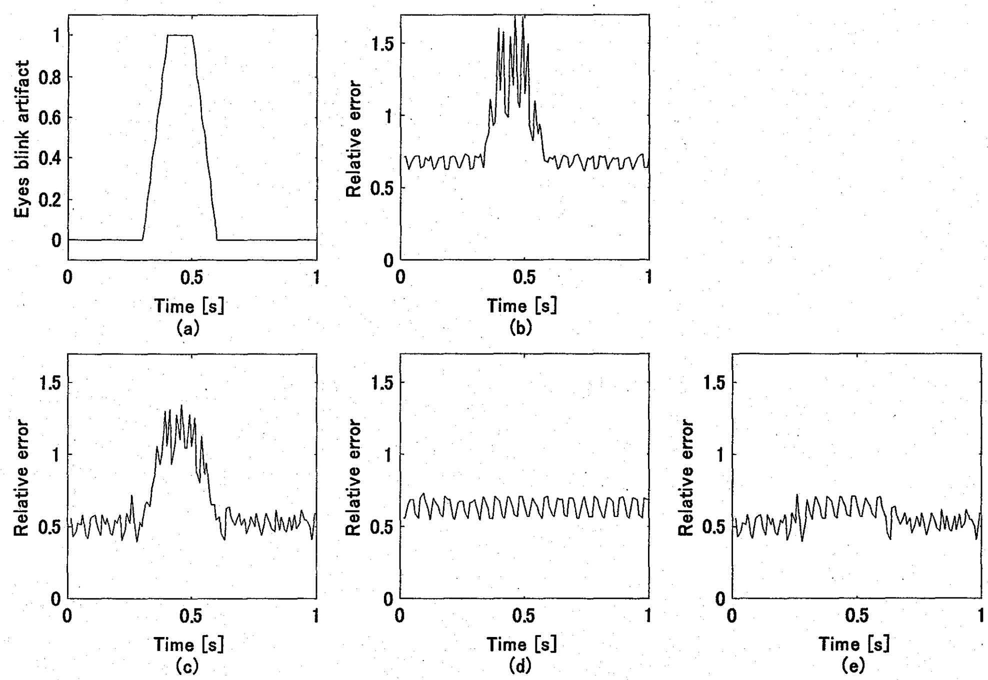

Fig. 3. Effects of time-varying PPFs. (a) Eyes blink artifact described in time domain. (b) The RE in the case of constant γ_k and constant Q_b of the background noise. (c) The RE in the case of time varying γ_k with constant Q_b of the background noise. (d) The RE in the case of time varying γ_k with constant Q_a of the eye blink artifact. (e) The RE in the case of time varying γ_k and Q_k.

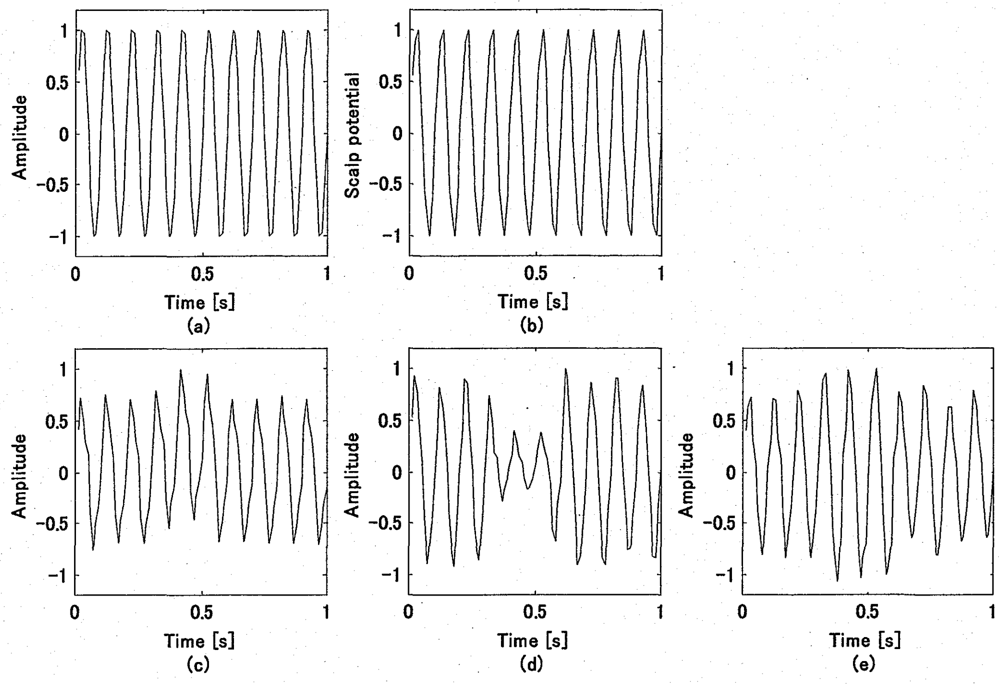

Fig. 4. (a) Normalized temporal variation of the actual source strength at the nearest point in space from an assumed dipole source over the DL surface. (b) Normalized temporal variation of the scalp potential at the nearest point in space from an assumed dipole source contaminated with the GWN. (c) Estimated temporal behavior of the source strength at the same point as (a) over the DL surface, obtained by means of the PPF with constant γ_k and constant Q_b. (d) Estimated temporal behavior of the source strength at the same point as (a) over the DL surface, obtained by means of the PPF with time variant γ_k and constant Q_b. (e) Estimated temporal behavior of the source strength at the same point as (a) over the DL surface, obtained by means of the PPF with time variant γ_k and Q_k.

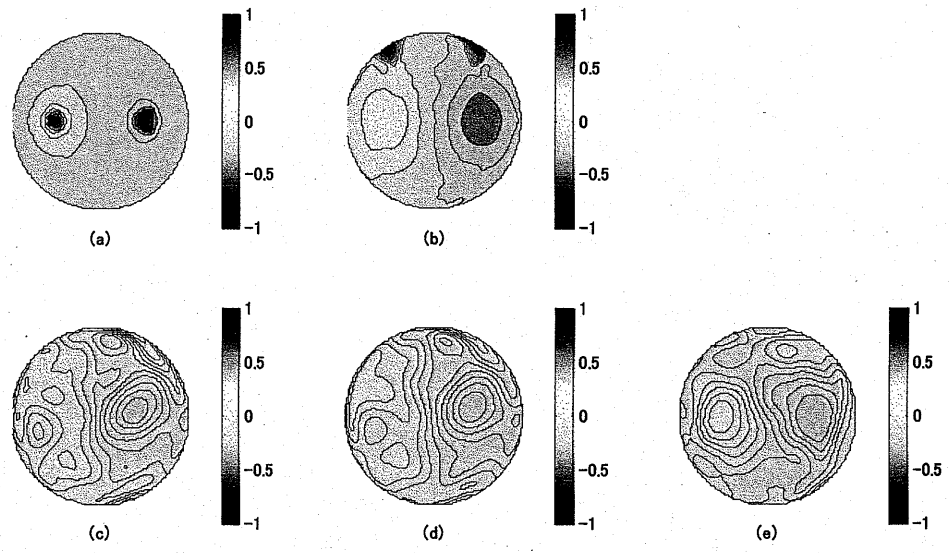

Fig. 5. One example of cortical DL imaging of two radial dipoles. (a) Actual DL distribution. (b) Scalp potential contaminated with artifact. (c) Estimated result of the PPF with constant γ_k and constant Q_b. (d) Estimated result with time variant γ_k and constant Q_b. (e) Estimated result with time variant γ_k and Q_k.

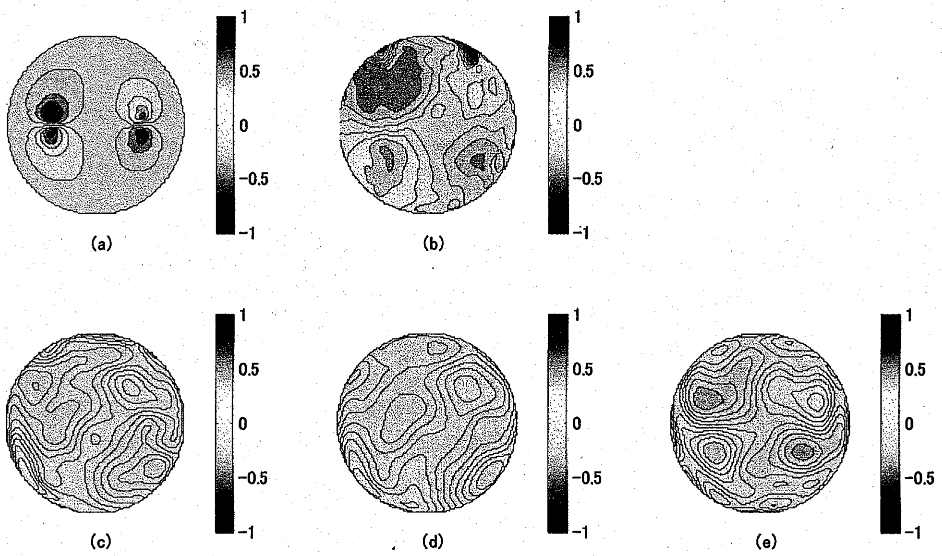

Fig. 6. One example of cortical DL imaging of two tangential dipoles. (a) Actual DL distribution. (b) Scalp potential contaminated with artifact. (c) Estimated result of the PPF with constant γ_k and constant Q_b. (d) Estimated result with time variant γ_k and constant Q_b. (e) Estimated result with time variant γ_k and Q_k.

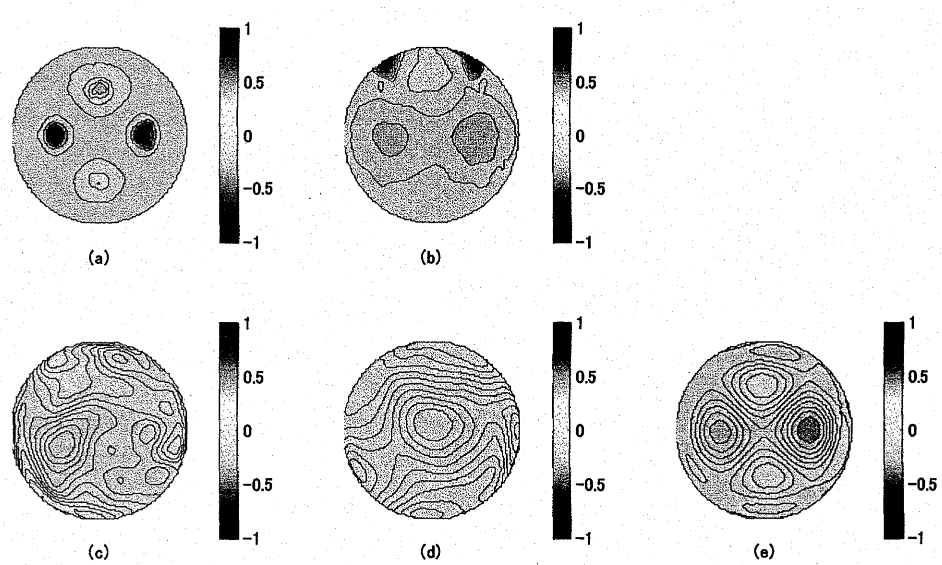

Fig. 7. One example of cortical DL imaging of four radial dipoles. (a) Actual DL distribution. (b) Scalp potential contaminated with artifact. (c) Estimated result of the PPF with constant γ_k and constant Q_b. (d) Estimated result with time variant γ_k and constant Q_b. (e) Estimated result with time variant γ_k and Q_k.

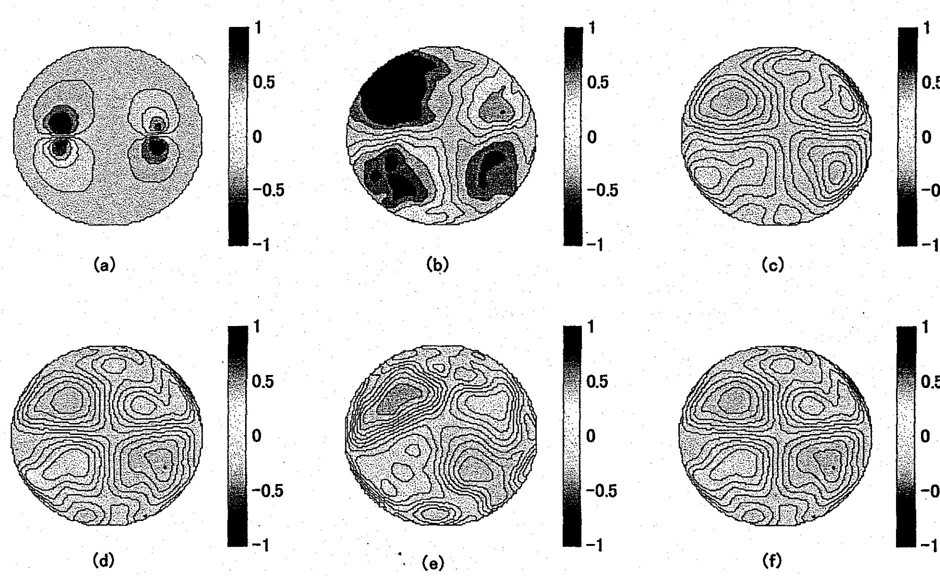

Fig. 8. One example of cortical DL imaging of two tangential dipoles without eye-blink artifact. (a) Actual DL distribution. (b) Scalp potential during background GWN. (c) Estimated result of the PPF with constant γ_k and constant Q_b of background GWN. (d) Estimated result with time variant γ_k and constant Q_b. (e) Estimated result with time variant γ_k and constant Q_a of eye-blink artifact. (f) Estimated result with time variant γ_k and Q_k.

APPENDIX

1. Hori, J. and He, B., Equivalent dipole source imaging of brain electric activity by means of parametric projection filter, Annals of Biomedical Engineering, vol.29, no.5, pp.436-445, 2001.
2. Hori, J. and He, B.,EEG Cortical potential imaging of brain electrical activity by means of parametric projection filters, IEICE Trans. Info. & Syst., vol.E86-D, no.9, pp.1909-1920, Sept. 2003.
3. Hori, J., Lian, J., and He, B., Cortical potential imaging of brain electrical activity by means of parametric projection filter, Methods Inform. Med., vol.43, no.1, pp.66-69, March 2004.
4. 宮田治，堀潤一，ダイポールイメージングによる脳内信号源の推定，信学技報，MBE2001-74, pp.23-30, Oct. 2001.
5. Hori, J., Lian, J., and He, B., Cortical potential imaging of brain electrical activity by means of parametric projection filter, Proc. 4th Int. Workshop Biosignal Interpretation, vol.4, 311-314, Italy, June 2002.
6. 大類稔，堀潤一，斉藤義明，B. He，信号と雑音の統計的性質を考慮した空間逆フィルタによる脳内ダイポールイメージング日本 ME 学会甲信越支部・北陸支部合同大会，pp.12-13, Aug. 2002.
7. 相場雅彰，堀潤一，斉藤義明，相場雅彰，パラメトリック射影フィルタを用いた時空間脳内ダイポールイメージング，日本 ME 学会甲信越支部・北陸支部合同大会，pp.27-28, Aug. 2002.
8. Hori, J., Lian, J., and He, B., Comparison between parametric Weiner filter and parametric projection filter in cortical equivalent dipole layer imaging,Proc. 2nd Joint EMBS/BMES Conf., vol.2, 929-930, Houston, Oct. 2002.
9. 堀潤一，脳内電気活動イメージングとその応用，第 12 回電気学会東京支部東京支部新潟支所研究発表会，pp.9-10, Nov. 2002（招待講演）.
10. 大島健志，堀潤一，斉藤義明，B. He，脳内ダイポールイメージングシステムの開発と誘発脳波への応用，第 18 回生体・生理工学シンポジウム論文集，pp.247-248, Oct. 2003.
11. Hori, J. and He, B.: "Artifact elimination in spatiotemporal cortical dipole layer imaging with parametric projection filter," 15th World Congress of the International Society of Brain Electromagnetic Topography, Urayasu, April 2004 (accepted).